

Self-Supervised Learning of Music-Dance Representation through Explicit-Implicit Rhythm Synchronization

Jiashuo Yu^{1,2,*}, Junfu Pu^{2,†}, Ying Cheng¹, Rui Feng^{1,†}, Ying Shan²

¹Fudan University ²ARC Lab, Tencent PCG

{jsyu19, chengy18, fengrui}@fudan.edu.cn, {jevinpu, yingsshan}@tencent.com

Abstract

Although audio-visual representation has been proved to be applicable in many downstream tasks, the representation of dancing videos, which is more specific and always accompanied by music with complex auditory contents, remains challenging and uninvestigated. Considering the intrinsic alignment between the cadent movement of dancer and music rhythm, we introduce **MuDaR**, a novel **Music-Dance Representation** learning framework to perform the synchronization of music and dance rhythms both in explicit and implicit ways. Specifically, we derive the dance rhythms based on visual appearance and motion cues inspired by the music rhythm analysis. Then the visual rhythms are temporally aligned with the music counterparts, which are extracted by the amplitude of sound intensity. Meanwhile, we exploit the implicit coherence of rhythms implied in audio and visual streams by contrastive learning. The model learns the joint embedding by predicting the temporal consistency between audio-visual pairs. The music-dance representation, together with the capability of detecting audio and visual rhythms, can further be applied to three downstream tasks: (a) dance classification, (b) music-dance retrieval, and (c) music-dance retargeting. Extensive experiments demonstrate that our proposed framework outperforms other self-supervised methods by a large margin.

1. Introduction

Recent years have witnessed the rapid growth of dancing video amounts on online video-sharing websites. The demand for automatically processing dancing videos based on content is thence becoming increasingly stronger. In literature, many prior works have achieved promising results on music-dance tasks, *e.g.*, music-driven dance generation [19, 23, 29, 54] and music-dance alignment [43]. However, these methods are usually task-specific and have a strong dependence on labeled data, which restricts their

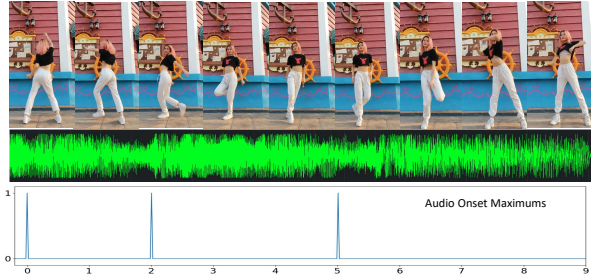


Figure 1. Illustration of a dancing clip with its corresponding audio rhythms. The motion of the dancer is in sync with the music rhythms, which means the starting keypoint of dancing motion lies on the temporal position of music onset maximum. The correlations between motion and onset features are used as explicit training signals, which together with the implicit rhythm consistency contribute to the self-supervised representation learning.

generalizability and applicability to a large extent.

A more practical way is to leverage the correlation between auditory and visual contents as the proxy to train task-agnostic models without human annotation. The derived representation can further be applied to a variety of downstream tasks with minor modifications. Though recent audio-visual pre-trained models [5, 6, 13, 14, 21, 26, 32, 37] have delivered impressive performance, these methods are not generalizable for dancing scenarios. The reason is that the visual contents of dancing videos consist of complex motions and characteristics. Meanwhile, dancing music, the auditory counterpart, embodies various attributes like lyrics, rhythms, tempos, etc. These fine-grained features are neglected by existing self-supervised audio-visual methods, leading to the consequence that meticulous conjunctions crossing modalities are not fully probed. As a result, a novel multimodal representation learning strategy is necessitated for dancing videos.

In this paper, we focus on the *rhythm* of dancing videos, which represents the amplitude of music intensity as well as the visual motions of dancers. As illustrated in Fig. 1, dancers tend to rhythmically move by music in the same frequency to make dances look more coordinated. Such tem-

*Jiashuo Yu is an intern in ARC Lab, Tencent PCG.

†Corresponding authors.

poral key moments of dancing motions are usually in sync with the music rhythms, which can be reflected by the audio onset features. Inspired by this insight, we argue that the pattern of dancing motions, termed as the *visual rhythms*, should be synchronous with music rhythms. This temporal correspondence between rhythms can further be utilized as the supervised signals for self-supervised learning.

Specifically, the synchronization of music and dance rhythms is conducted both explicitly and implicitly. We argue that rhythms are implied in the auditory and visual contents, thus we leverage the consistency between audio and visual streams to perform implicit rhythm alignment. Moreover, the audio onset, which refers to the beginning of a musical note, can be regarded as the music rhythm. In this work, we train the model to learn visual rhythms based on appearance and motion cues, which are expected to be aligned with music rhythms in an explicit way. Finally, the entire model is unified by joint training for the multi-modal representation as well as visual rhythm extraction. By leveraging the joint representation and visual rhythms, MuDaR can be applied to many downstream applications. We conduct experiments on three practical tasks: dance classification, music-dance retrieval, and music-dance retargeting. The comparison with other self-supervised audio-visual methods verifies the effectiveness of our framework.

The contributions are summarized as follows:

- We devise a novel self-supervised representation learning strategy for dancing videos, which performs the music-dance rhythm synchronization both in explicit and implicit ways.
- We propose a joint music-dance representation and a dance rhythm extractor favorable for music-dance understanding and re-creation tasks.
- Extensive experiments on three downstream tasks, *i.e.* dance classification, music-dance retrieval, and dance-music retargeting, verify the effectiveness and generalizability of our model on music-dance scenarios.

2. Related Works

Audio-visual representation learning aims to learn the multisensory embeddings favorable for downstream tasks. Several existing methods [2, 3, 5, 6, 13, 14, 26, 37] focus on the characteristics of auditory and visual streams in a given video. The audio and visual contents in videos are usually corresponding and synchronous, and these natural inter-modality correlations can be utilized as the supervisory signal for large-scale self-supervised training. Apart from such correspondence, some works focus on the discriminative information across the modalities. [4, 21] explore the intrinsic differences between modality-aware semantics and propose a cross-modal deep clustering method to perform

cross-modality supervision. [32] propose a cross-modal active contrastive coding strategy to fully explore the diversity between positive and negative samples. Moreover, some methods [1, 8, 17, 18, 22, 34, 51, 52] explore the relationship of visual dynamic motions and audio signals. The correspondence between dynamic motions of objects and sound sources can be used for self-supervised object detection. In this paper, we propose a unified framework to combine these knowledge priors above, where the temporal correspondence is utilized for implicit rhythm synchronization, and the dynamic motions corresponding to music are exploited for explicit rhythm keypoint alignment.

Dance with music is a fundamental and challenging video category, where the movements of dancers are complex and the patterns of music and dance are diverse. Hence, models are required to explore more detailed information by capturing fine-grained features. Attempts in the representation learning field focus on the uni-modal music embeddings [30, 44, 48–50, 53]. Since music can be handled as a sequence of tokens, an ordinary pipeline is to train pre-trained models that have achieved promising performance in natural language processing, such as BERT [16]. However, the embeddings of the visual counterpart: dancing, as well as the joint music-dance representation that captures cross-modal music-dance interactions, are rarely investigated. For the multimodal dance-music applications, many works [19, 23, 29, 54] tackle the problem of music-dance generation, that is, generating a sequence of dancing videos based on the given music. Some methods [43] work on the audio-visual alignment, which tries to align mismatched dancing and music streams by learning frame-level dense correspondence. The most relevant to our work is visual rhythm and beat prediction [15, 38, 46], where visual rhythms and beats are extracted based on dancing motions or dancer skeletons. In our paper, we ameliorate visual rhythm predictions by involving more characteristics, and further leverage the synchronization of rhythms as a training proxy for multimodal representation learning.

3. Approach

MuDaR conducts rhythm synchronization via a two-pathway architecture, and the illustration of our framework is shown in Fig. 2. Our model performs explicit synchronization via the temporal alignment between music and dance rhythm keypoints, while the implicit part is implemented by identifying the synchrony between audio and visual streams. The details of each part are introduced below.

3.1. Explicit Rhythm Synchronization

3.1.1 Music Rhythm Detection.

For the music rhythm, a straightforward idea is to utilize the onset feature, which indicates the sudden increase of music

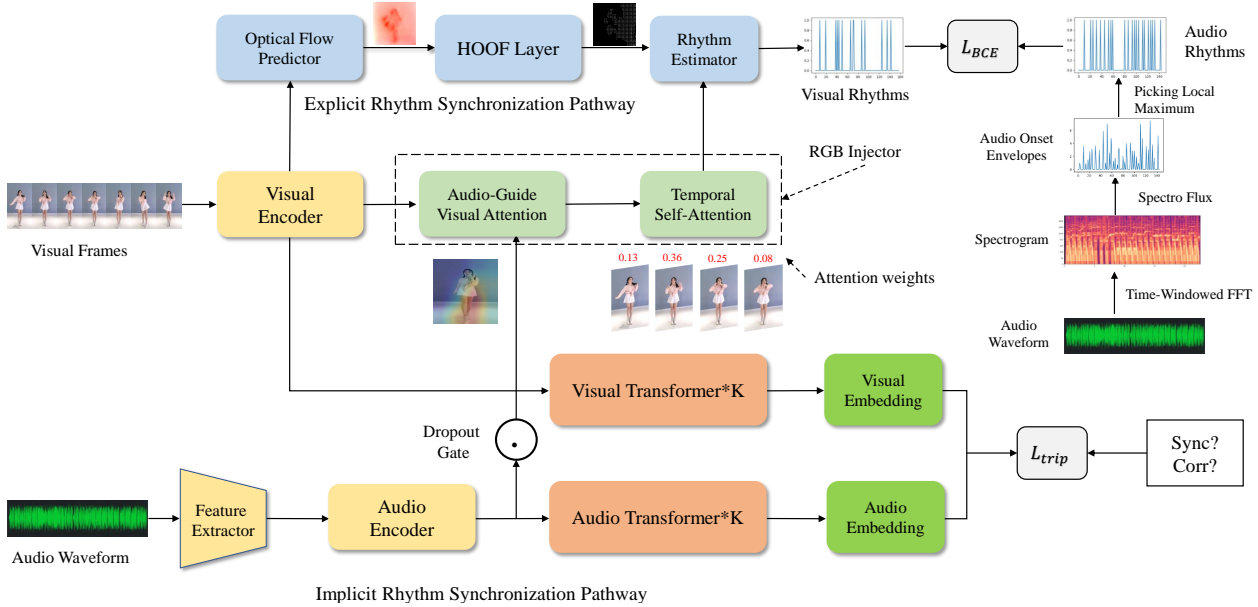


Figure 2. Illustration of our MuDaR framework. MuDaR involves two pathways: implicit and explicit music-dance synchronization. For the implicit pathway, we leverage the auditory and visual features to conduct corresponding and synchronization predictions with binary classification. For the other part, MuDaR explicitly learns visual rhythms based on the motions of dancers by performing temporal alignment with audio onsets, which can be viewed as the music rhythms. Two streams are trained jointly in a self-supervised manner.

volumes. Following [10], we first obtain the spectrograms by conducting time-windowed FFT to the audio signal represented as follows,

$$X(n, k) = \sum_{q=-\frac{N}{2}}^{\frac{N}{2}-1} v(hn + q)w(q)e^{-\frac{2j\pi qk}{N}}, \quad (1)$$

where $X(n, k)$ denotes the k^{th} frequency bin of temporal position n ; $v(\cdot)$ is the audio signal; h denotes the hop size; $w(\cdot)$ is the Hamming window, N is the time window size.

Then we compute the bin-wise difference between spectrograms to get the spectral flux, which indicates the magnitude of audio signals. The onset envelope, a positive 1D feature, is computed by summing the positive spectral flux:

$$OE(n) = \sum_{k=-\frac{N}{2}}^{\frac{N}{2}-1} \max(0, |X(n, k)| - |X_{ref}(n - \mu, k)|), \quad (2)$$

where n, k denotes the temporal position and bin number, respectively; $OE(n)$ is the onset envelope at time step n ; X_{ref} denotes the maximum-filtered spectrogram proposed in [10]; μ is the time lag.

Finally, we pick the local maximum of the onset envelope to detect the discrete onset feature. The local maximum will be selected as an onset only if it is some threshold above the local average value. The entire rhythm extraction procedure can be derived by the python package LibROSA [33] with the default hyperparameter settings for all algorithms mentioned above.

3.1.2 Dance Rhythm Detection.

For the dancing rhythms, we focus on the motion characteristics of dancers based on dense optical flow estimation.

Optical flow estimator. Optical flow indicates the direction and magnitudes of visual motions. Therefore, we estimate the dense optical flows as the initial step of dance rhythm detection. The effective, lightweight PWC-Net [41] is selected as the backbone optical flow network. To be specific, PWC-Net extracts feature maps in different resolutions via a feature pyramid extractor consisting of several stacking convolution layers, then warps features of the current frame toward the previous frame and constructs a cost volume. Finally, the optical flow is predicted by a multi-layer CNN estimator and refined by a dilated context network.

Histograms of Optical Flow. Though some existing methods estimate visual trajectory by dense optical flows [18, 51], these trajectories live in the Euclidean space, thereby highly relying on the constant of camera view. On the contrary, we utilize the Histogram of Oriented Optical Flow (HOOF) [12], a non-Euclidean feature, to represent motions in a non-linear manifold. HOOF is independent of the camera directions, amplification of camera view, and background noise, which is more robust and generalizable for more dancing scenarios. Specifically, HOOF is computed by the weighted summation of the magnitude of optical flow, where the optical flow $v(t, x, y)$ in each time-stamp is separated into n bins according to its angle from

the horizontal axis, represented as follows:

$$H(n, k) = \sum_{x, y} M_t(x, y) \mathbb{1}_\theta(P_t(x, y)), \quad (3)$$

$$\mathbb{1}_\theta(\phi) := \begin{cases} 1, & \text{if } |\theta - \phi| \leq \frac{2\pi}{B}, \\ 0, & \text{otherwise,} \end{cases} \quad (4)$$

where $M_t(x, y) \in \mathbb{R}^{H \times W}$ denotes the magnitude of optical flow in t^{th} time, which is computed by $\sqrt{x^2 + y^2}$; $P(t) \in \mathbb{R}^{H \times W}$ indicating the angle of optical flow with x-axis in time step t is calculated by $\tan^{-1} \frac{y}{x}$, $\mathbb{1}_\theta(\phi)$ is an indicator function; and B denotes the total number of bins.

RGB injector. A straightforward way to predict visual rhythms is directly use HOOF for visual rhythm estimation. However, this could lead the prediction to be highly dependent on the quality of optical flow. Considering that the feature maps extracted from raw images may also contain contributing information, we propose an RGB injector to infuse visual cue to motion features as an enhancement.

To be specific, we use the feature map f_{rgb} generated by the encoder of PWC-Net [41] in the explicit rhythm synchronization pathway. Then f_{rgb} is tiled and projected by a linear layer to reduce the dimensionality. To highlight the rhythm keypoints in the temporal dimension, we introduce the long-range temporal interactions by the multi-head self-attention mechanism [42]. The refined visual features are put into the visual rhythm estimator as the infusion.

We also argue that the inherent coherence of music-dance signals can be utilized for visual rhythm prediction. The audio-guided spatial-channel attention mechanism [47] is leveraged to explore the relationship between auditory and visual features. We use audio features f_a extracted by the audio encoder of the implicit rhythm synchronization pathway (which will be introduced in Sec. 3.2), and the audio-guided visual features can be computed as follows,

$$w_{a:rgb}^c = \sigma(W_1 U_1^c(\rho_a(f_a \odot U_{rgb}^c(f_{rgb})))), \quad (5)$$

$$f_{a:rgb}^c = \sum_{i=1}^k w_{a:rgb}^{c:i} f_{rgb}^i, \quad (6)$$

$$w_{a:rgb}^s = \text{softmax}(\delta(W_2(U_a^s(f_a) \odot U_{rgb}^s(f_{rgb})))), \quad (7)$$

$$f_{a:rgb}^s = \sum_{i=1}^k w_{a:rgb}^{s:i} f_{rgb}^i, \quad (8)$$

where U_{rgb}^c, U_{rgb}^s are linear layers with non-linearity activation; W_1, W_2 are learnable parameters; σ indicate the sigmoid function; ρ denotes global average pooling; δ is the hyperbolic tangent function; and $w_{a:rgb}^c, w_{a:rgb}^s$ are the channel and spatial attention map, respectively.

However, the prediction of dance rhythms cannot rely on the corresponding music when applied to downstream tasks. The performance significantly declines when audio signals are available during training while missing in inference. To

address this problem, we refer to Dropout [40], a simple yet effective method which initial goal is to prevent model from being dependent on some specific neurons. Inspired by this paradigm, we propose an audio dropout gate, which randomly drops partial auditory inputs in a mini-batch with constant ratios during training. To this end, MuDaR is capable of detecting visual rhythms both with and without music. The entire procedure can be formulated as:

$$f_{rgb1}, f_{rgb2} = \text{AudioDropout}(f_{rgb}, p), \quad (9)$$

$$\text{AudioDropout}(f, p) = f[b * p :], f[: b * p], \quad (10)$$

$$f_{a:rgb1} = \text{AGVA}(f_{rgb1}, f_a), \quad (11)$$

$$f'_{rgb2} = \text{Linear}(\text{Tile}(f_{rgb2})), \quad (12)$$

$$f_{a:rgb} = \text{Concat}(f_{a:rgb1}, f'_{rgb2}), \quad (13)$$

$$f_{inj} = \text{Att}(f_{a:rgb}, f_{a:rgb}, f_{a:rgb}), \quad (14)$$

where f_{inj} denotes the output of the RGB injector; AGVA denotes the audio-guided visual attention introduced in Eq.(5)~(8); Att denotes the multi-head self-attention; b denotes the mini-batch size; and p is the audio dropout rate.

Visual rhythm estimator. To explore the magnitude of visual appearance, we compute the first-order difference of motion features and RGB features, which are further combined with linear projection. Then a linear layer with non-linear activation is used for binary classification,

$$p_t^e = \sigma(W_e(U_{mot} f'_{mot} \oplus U_{inj} f'_{inj}) + b_e), \quad (15)$$

where f'_{mot}, f'_{inj} are the first-order difference of motion and injected features; U_{mot}, U_{inj} are linear layers with ReLU [36] activation; \oplus denotes concatenation across the channel dimension; W_e, b_e are parameters of linear classifier; σ denotes the sigmoid function.

3.2. Implicit Rhythm Synchronization

We claim that rhythms of music and dance are implied in the auditory and visual features, and the synchronization of music and dance streams can also be considered as the implicit version of rhythm synchronization. Following [1, 13, 26, 37], we employ Audio-Visual Correspondence (AVC) and Audio-Visual Temporal Synchronization (AVTS) as the pretext tasks for representation learning. Specifically, we leverage the raw videos as the positive samples, while creating asynchronous samples by performing temporal shifts and creating uncorrelated samples via combining visual and audio streams from different videos. Then the model is required to predict whether the assembled sample is synchronous (for AVTS) and corresponding (for AVC) or not, thereby performing self-supervised training.

One problem of this unsupervised paradigm is the construction of *false-negative samples*. For the AVC task, if we randomly sample a sequence of music that is the same as the raw dancing video, the newly-assembled sample is

actually music-dance corresponding. To address this problem, we compute the *rhythm similarity score* of the raw and newly selected audio streams by calculating the coincidence of rhythm positions, which is formulated as follows:

$$s_{rhy} = \sum_{t=1}^T |O_{pos}^t - O_{neg}^t| - \alpha T, \quad (16)$$

where s_{rhy} is the rhythm similarity score; O_{pos}^t denotes the positive music onset features; O_{neg}^t indicates the negative onsets; T denotes the length of dancing videos; $\alpha \in [0, 1]$ is a threshold hyperparameter. The negative sample will be selected only when the score is positive. For the AVTS task, the rhythms of dancing videos are sometimes periodic. Therefore, if we shift the current rhythm point exactly to another point afterward, the rhythms of audio and visual streams are re-aligned with certain time-lagged. To this end, we conduct additional constraints to prevent the shifted size from being the multiple of rhythm interval. Though the rhythm interval tends to be diverse, most onset peaks are concurrent with music beats, which are distributed with a constant temporal gap. In our work, the eighth note (quarter) is selected as the basic beat unit, and the shifted number of visual frames f_{sft} cannot be the multiple of the frame number identical to an eighth note,

$$f_{sft} \bmod (k_{fps} * \frac{60}{k_{bpm}} * \frac{1}{2}) \neq 0, \quad (17)$$

where k_{fps} denotes the frame sample rate; k_{bpm} denotes the number of quarter note (crotchet) per minute. Since we use the eighth note as the base beat unit, the number of beat units per minute will be $2 * k_{bpm}/60$.

After performing sampling constraints, the implicit rhythm synchronization can be trained in a self-supervised manner. To perform coherent optimization, we leverage the pyramid encoder of the PWC-Net as the visual encoder, and the last feature map of the pyramid output is kept as the visual feature. We also build a similar audio encoder including several 2D convolution layers. Then auditory and visual features are put into K stacking transformer [42] layers, respectively. We do not involve any modality interaction to make our framework generalizable for single-modality downstream tasks. Each transformer layer is constructed by the encoder part of the raw transformer architecture [42], including the multi-head self-attention, feed-forward layer, layer normalization [7], and residual connection [20]. In the self-attention block, features are temporally interacted to fully explore the long-range temporal correlation. Finally, triplet loss [39] is used for the refined auditory and visual features, which enlarges the distance between visual features and negative auditory features, while reducing the gap between visual features and positive audio features.

3.3. Optimization

For the implicit synchronization, using a classifier to predict binary logits and adopt the binary cross-entropy loss as the learning objective is a natural way for the AVC and AVTS tasks. However, this method suffers from the difficulty of training convergence. Some prior methods [14, 26, 32] opt to the contrastive loss as a substitution. In this work, the dense optical flow estimation requires high computation cost, thus the performance will be limited when the batch size is small. In this paper, we choose the triplet loss [39] with offline negative sample strategy. Specifically, we put a pair of positive audio and visual samples into the two-stream implicit synchronization pathway. Then we choose the negative audio samples from the whole dataset, which is brought into the audio streams together with the positive audio sample. The triplet loss function tries to make the refined positive audio feature $f'_{a:pos}$ closer to the refined visual features f'_v , while enlarge the distance between negative audio features $f'_{a:neg}$ and f'_v ,

$$\mathcal{L}^{im} = \sum_{i=1}^N \left[\|f'_v - f'_{a:pos}\|_2^2 - \|f'_v - f'_{a:neg}\|_2^2 + \alpha \right]_+, \quad (18)$$

where \mathcal{L}^{im} denotes the implicit loss, α is the margin between positive and negative pairs; $[\cdot]_+$ denotes picking the positive results, and N denotes the number of triplet pairs.

For the explicit synchronization, the straightforward way of using binary cross-entropy loss may cause overwhelming negative predictions during training due to the unbalanced distribution of rhythm and non-rhythm temporal keypoints. To address this problem, we adopt the focal loss proposed by [31]. Focal loss addresses the class imbalance by introducing a weighting hyperparameter α , and focuses more on hard samples rather than easier ones via the focusing parameter γ . The explicit loss \mathcal{L}^{ex} can be formulated as,

$$\mathcal{L}^{ex} = -\alpha_t (1 - p_t^e)^\gamma \log(p_t^e), \quad (19)$$

where p_t is the visual rhythm prediction.

Finally, the optimization is conducted in a joint-training manner, the overall objective function is formulated as,

$$\mathcal{L} = \lambda_1 \mathcal{L}^{im} + \lambda_2 \frac{1}{N} \sum_{t=1}^N \mathcal{L}_t^{ex}, \quad (20)$$

where λ_1, λ_2 are hyper-parameters, which indicate the weighted summation of these loss terms, N is the number of frames in each video.

4. Experiments

In this section, we first introduce the implementation details and ablation results of the self-supervised representation learning process. Then we conduct experiments on three downstream tasks: dance classification, music-dance retrieval, and music-dance retargeting.

4.1. Music-Dance Representation Learning

Approach	Data Size	Recall	Precision
MuDaR w/ BCE	190k	82.2%	37.0%
MuDaR w/ regression	190k	43.8%	51.9%
MuDaR w/ CRF	190k	70.2%	79.8%
MuDaR (full)	47k	59.6%	73.1%
MuDaR (full)	140k	71.4%	78.9%
MuDaR (full)	190k	73.2%	82.0%

Table 1. The evaluation of visual rhythm prediction compared with two ablated models. We also report the performance of our full model with different dataset sizes.

Dataset. MuDaR can be trained by large-scale dancing videos without any annotation. The only requirement for unlabeled data is that dancers should twist their bodies following the rhythms of music, which is a fundamental rule for dancing. In this paper, we collect 194,407 dancing videos from an information feed platform and online video-sharing application. The training data can be separated into four categories, *i.e.* dancing with pop music, hip-hop, modern dance, and K-pop, with nearly equal proportions. These category labels are unnecessary during the training and inference phase.

Implementation details. All dancing videos are cropped to 8s clips. To remove background noises, we discard the beginning and ending part of each dance, and select 4 seconds before the middle of the video together with 4 seconds after. Visual frames are sampled with a frame rate of 8 fps. Then frames are resized to 256×256. To maintain the camera view unchanged, we do not apply any visual transformation for data augmentation. Audios are sampled with a sample rate of 16kHz, and we extract Mel-spectrograms, onset envelopes, onset maximum, beat, and tempograms using the python package LibROSA [33]. For the implicit synchronization pathway, the audio inputs are the concatenation of Mel-spectrograms, beat, onset envelopes, and tempograms, while the onset maximums are used as the ground-truth of rhythms for the explicit synchronization. We use Adam [25] optimizer with the initial learning rate of 1e-4. The entire model is trained on 64 NVIDIA Tesla V100 GPUs for 50 epochs with a batch size of 384. For the implicit synchronization, we adopt the curriculum learning strategy as [26]. AVC is used for the first 35 epochs, while the more challenging pretext task AVTS is used for the rest of the training process. More details are complemented in Appendix A.

Evaluation of MuDaR. We randomly sample 4,407 videos of the original 194,407 videos for evaluation, while using the remaining 190k videos for self-supervised training. To fully investigate the performance of the explicit rhythm pathway, we propose three ablated models for comparison. “MuDaR w/ CRF” denotes an ablated model that replaces

the binary prediction layer with a BiLSTM-CRF [28] layer, which is composed of a bidirectional long-short memory network [24] and a conditional random field [27] module. This ablated model regards the visual rhythm prediction task as a sequence labeling problem and considers the inner relationship of the consecutive frames. “MuDaR w/ regression” takes the visual rhythm prediction task as a regression problem. Instead of using local maximum over onset envelopes as the audio ground-truth, it directly minimizes the distance between model output and the onset envelope curve. The visual rhythms are then generated by picking the local maximum of the model output. “MuDaR w/ regression” replaces the binary focal loss with the raw binary cross-entropy loss. As shown in Tab. 1, we report recall and precision as the evaluation metrics. Results show that “MuDaR w/ BCE” achieves higher recall compared with raw MuDaR, while obtaining low precision, proving that the cross-entropy loss suffers from the imbalanced class distribution. “MuDaR w/ regression” achieves poor performance on all metrics. We argue that though the temporal position of music and dance rhythms are coincident, it’s illogical to force the intensity of visual rhythms to be identical to the audio rhythms. On the contrary, the full MuDaR model achieves promising results with respect to all metrics, showing the effectiveness of detecting visual rhythms. “MuDaR w/ CRF” performs slightly worse than the full model. This suggests that the BiLSTM-CRF layer performs unsatisfied when there are only two unbalanced categories for sequence labeling. More ablation studies are listed in Appendix B.

4.2. Dance Classification

Downstream architecture. We first evaluate the performance of MuDaR on the task of dance classification. To fully utilize the outputs of MuDaR (audio and visual embeddings, visual rhythms), we concatenate the visual embeddings and rhythms as visual outputs, and the auditory embeddings and onset as audio outputs. Then the audio and visual output features are put into a two-stream classifier. To be specific, audio and visual features are first put into two fully-connected layers with non-linear activation. Then the audio and visual features are concatenated and integrated by temporal pooling. Another two fully-connected layers with non-linearity are used for prediction.

Dataset. We evaluate the performance of dance classification on the Let’s Dance [11] dataset. This dataset contains more than 1,400 10-second dancing videos on a variety of 16 dance categories. Since a small part of the videos are unavailable on the Internet, we downloaded 1,262 dancing videos and randomly split the training, validation, and testing set with the proportion of 80%/10%/10% following [11, 45]. We employ the same data preprocessing procedure as the self-supervised representation training.

Implementation details. We train our network using

Approach	Data Size	Accuracy	Manner
Castro et al. [11]	/	70.2%	Supervised
MDR [45]	/	77.0%	Supervised
Multisensory [37]	190k	71.4%	S-Sup.+ ft
AVTS [26]	190k	68.3%	S-Sup.+ ft
LLA [13]	190k	73.0%	S-Sup.+ ft
MuDaR (full)	47k	76.1%	S-Sup.+ ft
MuDaR (full)	140k	79.4%	S-Sup.+ ft
MuDaR w/o rhy	190k	80.8%	S-Sup.+ ft
MuDaR (full)	190k	81.7%	S-Sup.+ ft

Table 2. The dance classification accuracy on Let’s Dance [11] dataset. “S-Sup.+ ft” denotes models pretrained on the self-supervised music-dance dataset, and then fine-tuned on the dance classification dataset.

Adam [25] optimizer with the initial learning rate of 4e-3, which is degraded by 10 after 20 and 50 epochs. The model is trained with a batch size of 64 for 70 epochs.

Experimental results. We compare MuDaR with two supervised methods: Temporal Three-Stream CNN [11] and Multimodal Dance Recognition [45]. To make a fair comparison, we also re-implement three audio-visual self-supervised methods: Multisensory [37], AVTS [26], and LLA [13], which are trained on the same large-scale dancing dataset used for MuDaR. Results shown in Tab. 2 indicate that our model outperforms all self-supervised baselines by a large margin. Moreover, the performance on the full pre-trained dataset (190k) surpasses the state-of-the-art supervised methods, showing the effectiveness of our representation learning framework on this downstream task. We also conduct ablation studies by removing the visual and auditory rhythms. Results show that MuDaR performs slightly worse without rhythm involvement. However, the decline is not significant, indicating the performance of dance classification mainly depends on the embeddings generated by the implicit synchronization pathway.

4.3. Music-Dance Retrieval

Downstream architecture. We also evaluate our model on the music-dance retrieval task. For the cross-modal retrieval, we compute the similarity scores of rhythms and embeddings, respectively. To be specific, for the embedding E_a, E_v and rhythm R_a, R_v , we compute the embedding similarity matrix S_e consisting of similarity scores of E_a and E_v , then compute the rhythm similarity matrix S_r via R_a and R_v . Finally, the hybrid similarity matrix can be computed by the weighted summation of S_e and S_r :

$$S_{hyb} = \lambda_3 S_e + (1 - \lambda_3) S_r, \quad (21)$$

where λ_3 is the hyperparameter. The top-K indices of the

Approach	Data Size	R@1	R@5	P@10	mAP
Multisensory [37]	190k	0.468	0.732	0.480	0.541
AVTS [26]	190k	0.430	0.698	0.467	0.484
LLA [13]	190k	0.501	0.781	0.512	0.576
MuDaR (full)	47k	0.532	0.782	0.596	0.573
MuDaR (full)	140k	0.604	0.894	0.632	0.622
MuDaR w/o rhy	190k	0.586	0.872	0.615	0.601
MuDaR (full)	190k	0.622	0.924	0.661	0.633

Table 3. Evaluation of music-dance retrieval of our framework compared with other self-supervised methods. MuDaR w/o rhy denotes the ablated model without rhythm involvement.

hybrid matrix are preserved as the retrieval result.

Dataset and task formulation. We conduct experiments on the Dance-50 [43] dataset for cross-modal retrieval. Dance-50 contains 50 hours of K-pop dancing videos collected from online video platforms. This dataset is originally used for audio-visual alignment without any category annotation available. To perform music-dance retrieval, we selected 22 dance music appeared with high frequency, where each song corresponds to 15-40 dancing videos from different dancers. We collected 400 labeled videos in total while using another 1833 unlabeled dances as the irrelevant data in the retrieval database. Since dances in the Dance-50 dataset are long videos of more than 30 seconds, we pre-process each annotated video by clipping 24 seconds from the beginning. For the unlabelled videos, we separated each video into several 24s dance clips. In this way, we got 400 labeled and 4,066 unlabeled dancing clips as the retrieval dataset. The objective of this task is to retrieve all related dances given the targeted music.

Experimental results. We leverage the self-supervised methods Multisensory [37], AVTS [26], and LLA [13] as baselines. For these baselines, since visual rhythms are unavailable, we only use the similarity matrix between embeddings for retrieval. We also investigate the role of visual rhythms via the ablated model “MuDaR w/o rhy”, and we report average top-k retrieval performance (R@K), top-k precision (P@K), and mAP as the evaluation metrics. As shown in Tab. 3, results show that MuDaR outperforms all baselines by a large margin. Our framework outperforms baseline LLA by 15% on R@5 and P@10, and 6% on mAP, which shows the effectiveness of our music-dance framework. Besides, the performance significantly declines after removing the rhythm information, indicating that rhythms are favorable for cross-modal retrieval.

4.4. Music-Dance Retargeting

Task Formulation. Music-dance retargeting aims to synthesize a new dancing video via two mismatched music and

dance clips. This task can be combined with the music-dance retrieval task as an automatic soundtrack generator, which synthesizes rhythm-aligned dancing videos after obtaining related music via cross-modal retrieval. Concretely, given a sequence of visual frames V , and a music clip A from different dancing videos, the objective of music-dance retargeting is to combine V and A into a natural new dancing video. This task evaluates the performance of rhythm extraction thoroughly, since we conduct the retargeting by warping the visual rhythms R_v into the alignment with the auditory counterpart R_a .

Downstream architecture. Due to the difference between the temporal lengths of V and A , we try to align as many rhythm points as possible via acceleration and shifting. We propose three retargeting patterns: temporal shifting, temporal acceleration, and dynamic temporal warping. For the temporal shifting, we propose a sliding window which size is equal to the length of the shorter sequence, and put it on the rhythm of longer duration. We reserve the cropped clip with the most similar number of rhythm points, then align the starting rhythm points of two sequences. The second pattern is temporal acceleration, where we compute the temporal interval I between two adjacent rhythm points: $I_k^m = P_{k+1}^m - P_k^m$, where $m \in \{a, v\}$ denotes the modality index, k indicates the rhythm keypoint index, and P_k^m denotes the temporal position of the k^{th} rhythm in the modality m . Then we manage to make I_k^v and I_k^a equal for all rhythm indices by interpolating and removing visual frames. The third manner is dynamic temporal warping (DTW) [9, 35], which is capable of selecting the most suitable aligning strategy. Specifically, DTW aims to find the optimal warping path that aligns R_v and R_a with minimum rhythm mismatch cost, which is defined by the accumulated distance between the rhythm keypoints. The cumulative distance c in position (i, j) can be computed using dynamic programming:

$$c(i, j) = d(i, j) + M\{c(i-1, j-1), c(i-1, j), c(i, j-1)\}, \quad (22)$$

$$d(i, j) = |P_i - P_j|, \quad (23)$$

where $M(\cdot)$ denotes the minimize function; i, j are indices of rhythms; P_i denotes the temporal position of the i^{th} rhythm point. The warping path determines the detailed frame accelerate strategy with minimum warping costs, thereby resulting in optimal retargeting performance.

Qualitative results. Since there is no feasible quantitative metric for music-dance retargeting, we provide some qualitative results to show the performance of our method as shown in Fig. 3. All dancing videos are randomly selected from the test set of the representation learning dataset. For the synthetic videos by temporal shifting, the inner rhythm may be mismatched for we only perform alignment on the first rhythm points, which makes the synthetic video uncoordinated. Besides, the performance is unsatisfactory when



Figure 3. Qualitative results of three methods on the music-dance retargeting task. Frames with colored boxes denote visual rhythm positions. Results show that videos synthesized by DTW achieve both optimal rhythm alignment and satisfactory viewing fluency.

the temporal lengths of audio and visual clips are similar, since the range of temporal offset is highly limited. Retargeting videos by temporal acceleration may lead some parts of the synthetic video to be extremely fast or slow. This is because when the gap between I_k^v and I_k^a is quite large, we need to interpolate or remove a large number of visual frames, which seriously affects the viewing fluency. On the contrary, the synthetic video by DTW achieves excellent rhythm alignment compared with videos generated by temporal shifting, and the synthetic frames are more consistent than the temporal acceleration production. *We provide more synthetic video demos, including raw audio and visual clips in the supplementary material.*

5. Conclusion

In this paper, we propose a novel self-supervised Music-Dance Representation learning framework via the synchronization of music and dance rhythms both explicitly and implicitly. We first explicitly extract and align the visual and auditory rhythms of the dancing videos based on the magnitudes of dancer motions and music contents. This part of the framework can also be utilized as a dancing rhythm extractor. We then leverage the contrastive learning strategy to synchronize the auditory and visual streams of the dancing videos, which can also be viewed as an implicit music-dance rhythm synchronization. Our model outperforms other self-supervised methods in downstream tasks by a large margin, verifying the effectiveness of our framework from both the video understanding and re-creation perspectives. We hope our work could arouse the gorgeous growth of works on music-dance self-supervised learning, and we believe the paradigm and benchmarks we proposed can lead to more meaningful dance-music researches.

References

- [1] Triantafyllos Afouras, Yuki M Asano, Francois Fagan, Andrea Vedaldi, and Florian Metz. Self-supervised object detection from audio-visual correspondence. *arXiv preprint arXiv:2104.06401*, 2021. [2](#), [4](#)
- [2] Triantafyllos Afouras, Andrew Owens, Joon Son Chung, and Andrew Zisserman. Self-supervised learning of audio-visual objects from video. In *ECCV*, 2020. [2](#)
- [3] Jean-Baptiste Alayrac, Adrià Recasens, Rosalia Schneider, Relja Arandjelović, Jason Ramapuram, Jeffrey De Fauw, Lucas Smaira, Sander Dieleman, and Andrew Zisserman. Self-supervised multimodal versatile networks. *arXiv preprint arXiv:2006.16228*, 2020. [2](#)
- [4] Humam Alwassel, Dhruv Mahajan, Bruno Korbar, Lorenzo Torresani, Bernard Ghanem, and Du Tran. Self-supervised learning by cross-modal audio-video clustering. In *NeurIPS*, volume 33, 2020. [2](#)
- [5] Relja Arandjelovic and Andrew Zisserman. Look, listen and learn. In *ICCV*, pages 609–617, 2017. [1](#), [2](#)
- [6] Relja Arandjelovic and Andrew Zisserman. Objects that sound. In *ECCV*, pages 435–451, 2018. [1](#), [2](#)
- [7] Jimmy Lei Ba, Jamie Ryan Kiros, and Geoffrey E Hinton. Layer normalization. *arXiv preprint arXiv:1607.06450*, 2016. [5](#)
- [8] Zohar Barzelay and Yoav Y Schechner. Harmony in motion. In *CVPR*, pages 1–8, 2007. [2](#)
- [9] Donald J Berndt and James Clifford. Using dynamic time warping to find patterns in time series. In *KDD workshop*, volume 10, pages 359–370, 1994. [8](#)
- [10] Sebastian Böck and Gerhard Widmer. Maximum filter vibrato suppression for onset detection. In *DAFx*, volume 7, 2013. [3](#)
- [11] Daniel Castro, Steven Hickson, Patsorn Sangkloy, Bhavishya Mittal, Sean Dai, James Hays, and Irfan Essa. Let’s dance: Learning from online dance videos. *arXiv preprint arXiv:1801.07388*, 2018. [6](#), [7](#)
- [12] Rizwan Chaudhry, Avinash Ravichandran, Gregory Hager, and René Vidal. Histograms of oriented optical flow and binet-cauchy kernels on nonlinear dynamical systems for the recognition of human actions. In *CVPR*, pages 1932–1939, 2009. [3](#)
- [13] Ying Cheng, Ruize Wang, Zhihao Pan, Rui Feng, and Yuejie Zhang. Look, listen, and attend: Co-attention network for self-supervised audio-visual representation learning. In *ACM MM*, pages 3884–3892, 2020. [1](#), [2](#), [4](#), [7](#)
- [14] Joon Son Chung and Andrew Zisserman. Out of time: automated lip sync in the wild. In *ACCV*, pages 251–263, 2016. [1](#), [2](#), [5](#)
- [15] Abe Davis and Maneesh Agrawala. Visual rhythm and beat. In *CVPRW*, pages 2532–2535, 2018. [2](#)
- [16] Jacob Devlin, Ming-Wei Chang, Kenton Lee, and Kristina Toutanova. BERT: Pre-training of deep bidirectional transformers for language understanding. *arXiv preprint arXiv:1810.04805*, 2018. [2](#)
- [17] Chuang Gan, Deng Huang, Hang Zhao, Joshua B Tenenbaum, and Antonio Torralba. Music gesture for visual sound separation. In *CVPR*, pages 10478–10487, 2020. [2](#)
- [18] Chuang Gan, Hang Zhao, Peihao Chen, David Cox, and Antonio Torralba. Self-supervised moving vehicle tracking with stereo sound. In *ICCV*, pages 7053–7062, 2019. [2](#), [3](#)
- [19] Xin Guo, Yifan Zhao, and Jia Li. Danceit: Music-inspired dancing video synthesis. *TIP*, 2021. [1](#), [2](#)
- [20] Kaiming He, Xiangyu Zhang, Shaoqing Ren, and Jian Sun. Deep residual learning for image recognition. In *CVPR*, pages 770–778, 2016. [5](#)
- [21] Di Hu, Feiping Nie, and Xuelong Li. Deep multimodal clustering for unsupervised audiovisual learning. In *CVPR*, pages 9248–9257, 2019. [1](#), [2](#)
- [22] Di Hu, Rui Qian, Minyue Jiang, Xiao Tan, Shilei Wen, Errui Ding, Weiyao Lin, and Dejing Dou. Discriminative sounding objects localization via self-supervised audiovisual matching. In *NeurIPS*, volume 33, 2020. [2](#)
- [23] Ruozi Huang, Huang Hu, Wei Wu, Kei Sawada, Mi Zhang, and Daxin Jiang. Dance revolution: Long-term dance generation with music via curriculum learning. *arXiv preprint arXiv:2006.06119*, 2020. [1](#), [2](#)
- [24] Zhiheng Huang, Wei Xu, and Kai Yu. Bidirectional LSTM-CRF models for sequence tagging. *arXiv preprint arXiv:1508.01991*, 2015. [6](#)
- [25] Diederik P Kingma and Jimmy Ba. Adam: A method for stochastic optimization. *arXiv preprint arXiv:1412.6980*, 2014. [6](#), [7](#)
- [26] Bruno Korbar, Du Tran, and Lorenzo Torresani. Cooperative learning of audio and video models from self-supervised synchronization. In *NeurIPS*, page 7774–7785, Red Hook, NY, USA, 2018. [1](#), [2](#), [4](#), [5](#), [6](#), [7](#)
- [27] John D. Lafferty, Andrew McCallum, and Fernando C. N. Pereira. Conditional random fields: Probabilistic models for segmenting and labeling sequence data. In *ICML*, page 282–289, 2001. [6](#)
- [28] Guillaume Lample, Miguel Ballesteros, Sandeep Subramanian, Kazuya Kawakami, and Chris Dyer. Neural architectures for named entity recognition. *arXiv preprint arXiv:1603.01360*, 2016. [6](#)
- [29] Hsin-Ying Lee, Xiaodong Yang, Ming-Yu Liu, Ting-Chun Wang, Yu-Ding Lu, Ming-Hsuan Yang, and Jan Kautz. Dancing to music. *arXiv preprint arXiv:1911.02001*, 2019. [1](#), [2](#)
- [30] Hongru Liang, Wenqiang Lei, Paul Yaozhu Chan, Zhenglu Yang, Maosong Sun, and Tat-Seng Chua. Pirhdy: Learning pitch-, rhythm-, and dynamics-aware embeddings for symbolic music. In *ACM MM*, pages 574–582, 2020. [2](#)
- [31] Tsung-Yi Lin, Priya Goyal, Ross Girshick, Kaiming He, and Piotr Dollár. Focal loss for dense object detection. In *ICCV*, pages 2980–2988, 2017. [5](#)
- [32] Shuang Ma, Zhaoyang Zeng, Daniel McDuff, and Yale Song. Active contrastive learning of audio-visual video representations. In *ICLR*, 2021. [1](#), [2](#), [5](#)
- [33] Brian McFee, Colin Raffel, Dawen Liang, Daniel PW Ellis, Matt McVicar, Eric Battenberg, and Oriol Nieto. librosa: Audio and music signal analysis in python. In *python in science conference*, volume 8, pages 18–25, 2015. [3](#), [6](#)
- [34] Pedro Morgado, Yi Li, and Nuno Nvasconcelos. Learning representations from audio-visual spatial alignment. In *NeurIPS*, volume 33, 2020. [2](#)

- [35] Meinard Müller. Dynamic time warping. *Information retrieval for music and motion*, pages 69–84, 2007. 8
- [36] Vinod Nair and Geoffrey E Hinton. Rectified linear units improve restricted boltzmann machines. In *ICML*, 2010. 4
- [37] Andrew Owens and Alexei A Efros. Audio-visual scene analysis with self-supervised multisensory features. In *ECCV*, pages 631–648, 2018. 1, 2, 4, 7
- [38] Fabrizio Pedersoli and Masataka Goto. Dance beat tracking from visual information alone. In *Proc. Int. Soc. Music Inf. Retrieval Conf*, pages 400–408, 2020. 2
- [39] Florian Schroff, Dmitry Kalenichenko, and James Philbin. Facenet: A unified embedding for face recognition and clustering. In *CVPR*, pages 815–823, 2015. 5
- [40] Nitish Srivastava, Geoffrey Hinton, Alex Krizhevsky, Ilya Sutskever, and Ruslan Salakhutdinov. Dropout: a simple way to prevent neural networks from overfitting. *JMLR*, 15(1):1929–1958, 2014. 4
- [41] Deqing Sun, Xiaodong Yang, Ming-Yu Liu, and Jan Kautz. Pwc-net: Cnns for optical flow using pyramid, warping, and cost volume. In *CVPR*, pages 8934–8943, 2018. 3, 4
- [42] Ashish Vaswani, Noam Shazeer, Niki Parmar, Jakob Uszkoreit, Llion Jones, Aidan N Gomez, Łukasz Kaiser, and Illia Polosukhin. Attention is all you need. In *NeurIPS*, pages 5998–6008, 2017. 4, 5
- [43] Jianren Wang, Zhaoyuan Fang, and Hang Zhao. Alignnet: A unifying approach to audio-visual alignment. In *WACV*, pages 3309–3317, 2020. 1, 2, 7
- [44] Ho-Hsiang Wu, Magdalena Fuentes, and Juan P Bello. Exploring modality-agnostic representations for music classification. *arXiv preprint arXiv:2106.01149*, 2021. 2
- [45] Monika Wyszczanska and Tomasz Trzcinski. Multimodal dance recognition. In *VISIGRAPP*, pages 558–565, 2020. 6, 7
- [46] Yutong Xie, Haiyang Wang, Yan Hao, and Zihao Xu. Visual rhythm prediction with feature-aligning network. In *MVA*, pages 1–6, 2019. 2
- [47] Haoming Xu, Runhao Zeng, Qingyao Wu, Mingkui Tan, and Chuang Gan. Cross-modal relation-aware networks for audio-visual event localization. In *ACM MM*, pages 3893–3901, 2020. 4
- [48] Zijie Ye, Haozhe Wu, Jia Jia, Yaohua Bu, Wei Chen, Fanbo Meng, and Yanfeng Wang. Choreonet: Towards music to dance synthesis with choreographic action unit. In *ACM MM*, pages 744–752, 2020. 2
- [49] Mingliang Zeng, Xu Tan, Rui Wang, Zeqian Ju, Tao Qin, and Tie-Yan Liu. MusicBERT: Symbolic music understanding with large-scale pre-training. *arXiv preprint arXiv:2106.05630*, 2021. 2
- [50] Xinjian Zhang, Yi Xu, Su Yang, Longwen Gao, and Huyang Sun. Dance generation with style embedding: Learning and transferring latent representations of dance styles. *arXiv preprint arXiv:2104.14802*, 2021. 2
- [51] Hang Zhao, Chuang Gan, Wei-Chiu Ma, and Antonio Torralba. The sound of motions. In *ICCV*, pages 1735–1744, 2019. 2, 3
- [52] Hang Zhao, Chuang Gan, Andrew Rouditchenko, Carl Vondrick, Josh McDermott, and Antonio Torralba. The sound of pixels. In *ECCV*, September 2018. 2
- [53] Hongyuan Zhu, Ye Niu, Di Fu, and Hao Wang. MusicBERT: A self-supervised learning of music representation. In *ACM MM*, pages 3955–3963, 2021. 2
- [54] Wenlin Zhuang, Congyi Wang, Siyu Xia, Jinxiang Chai, and Yangang Wang. Music2dance: Dancenet for music-driven dance generation. *arXiv preprint arXiv:2002.03761*, 2020. 1, 2